

Apatite formation on carbon nanotubes

Tsukasa Akasaka^{a,*}, Fumio Watari^a, Yoshinori Sato^b, Kazuyuki Tohji^b

^a Department of Biomedical, Dental Materials and Engineering, Graduate School of Dental Medicine, Hokkaido University, Sapporo, 060-8586, Japan

^b Graduate School of Environmental Studies, Tohoku University, Sendai, 980-8579, Japan

Received 1 November 2004; received in revised form 28 February 2005; accepted 28 March 2005

Available online 29 November 2005

Abstract

Apatite coating on carbon nanotubes (CNTs) was done with a biomimetic coating method. The multi-walled CNTs (MWNTs) of curled shape with about 30 nm in diameter were immersed for 2 weeks in the simulated body fluid. Observation by scanning electron microscopy (SEM) showed the formation of apatite on the MWNTs surface. The clusters of spherules consisting of needle-shaped apatite crystallites were massively grown on the aggregated MWNTs. The crystallites of 100 nm in width and 200–500 nm in length were grown perpendicularly to the longitudinal direction and radially originating from a common center of a single MWNT. Thus, the architecture of crystalline apatite at nano-scale levels could be produced by simple method and the MWNT may be acting as core for initial crystallization of apatite.

© 2005 Elsevier B.V. All rights reserved.

Keywords: Carbon nanotubes; Biomimetic coating; Apatite

1. Introduction

Carbon nanotubes (CNTs) have been attracting considerable attention because of their unique physical properties and potential for a variety of applications. The modifications of CNTs have been extensively investigated because of their relevance in electrical, mechanical and biological applications [1–8]. Immobilization of various functional molecules on CNT has also been examined in past studies [9–12]. For biomedical applications, new modification methods to give biocompatibility are needed for achievement of various required designs [13,14].

Biom mineralization is a natural process in human being and animals, resulting in the formation of bones and teeth. Ca–P solution, such as the simulated body fluid (SBF), has been frequently used for the biomimetic Ca–P coating to increase the bioactivity, and has been successfully applied to implant materials for some special dental and medical cases [15–17].

Here we developed a biom mineralization method to produce the architecture of apatite crystallites at nano-scale levels on the surface of MWNTs.

2. Experiment

The MWNTs used in this study were obtained from NanoLab (Brighton, MA, USA). The MWNTs of curled shape with about 30 nm in diameter were produced by the chemical vapor deposition (CVD) method. The raw MWNTs were refluxed in 6 N HCl solution and then washed thoroughly with deionized water and completely dried. Typical SEM (HITACHI S-4000) images of purified MWNTs are shown in Fig. 1.

The MWNTs material was dispersed in calcium phosphate solutions at a concentration of 10 mg/l by ultrasonication for 10 min. Then, the apatite crystallites were grown by immersing the MWNTs at 37 °C for various periods up to 2 weeks. The composition of the calcium phosphate solutions is as follows.

Revised SBF (R-SBF): NaCl (866 mg/l), CaCl₂ (125 mg/l), K₂HPO₄ (803 mg/l), KH₂PO₄ (326 mg/l), KCl (625 mg/l), MgCl₂ (59 mg/l) containing NaF (22 mg/l) and the pH was adjusted to 7.2 using KOH and no precipitation was observed in the solution during the experimental period. Dulbecco's phosphate-buffered saline (PBS(+)): NaCl (8000 mg/l), CaCl₂ (100 mg/l), KH₂PO₄ (200 mg/l), Na₂HPO₄ (1150 mg/l), KCl (200 mg/l), MgCl₂ (47 mg/l) containing NaF (22 mg/l) and the pH was adjusted to 7.4 using KOH

* Corresponding author. Tel.: +81 11 706 4251; fax: +81 11 706 4251.

E-mail address: akasaka@den.hokudai.ac.jp (T. Akasaka).

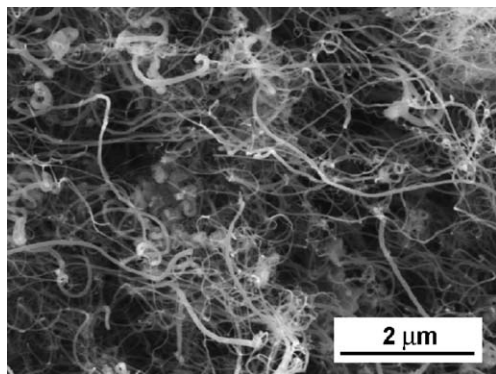


Fig. 1. SEM images of purified MWNTs.

and no precipitation was observed in the solution during the experimental period.

Standard SBF (S-SBF): NaCl (7996 mg/l), CaCl₂ (278 mg/l), K₂HPO₄ (174 mg/l), KCl (244 mg/l), NaHCO₃ (350 mg/l), MgCl₂ (143 mg/l), Na₂SO₄ (71 mg/l), (CH₂OH)₃CNH₂ (6057 mg/l), 1 M HCl (40 ml) containing NaF (22 mg/l) and the pH was adjusted to 7.4 using KOH.

Finally, the resultant MWNTs were separated from the suspension by filtration, gently washed with deionized water to remove impurities, and then dried at 60 °C for 6 h. In order to study the effects of immersing time-course on apatite growth, they were immersed for 6 h, 1 day, 2 days, and 2 weeks. To compare the influence of the substrates, we also use a square piece of carbon plate (10 × 10 × 1 mm³) (Nirako, Japan) instead of MWNTs.

The formation of apatite on the MWNTs surface was investigated by SEM after coating with carbon. Transmission infrared spectra were performed by the KBr method using a fourier transmission infrared spectrometer (FT-IR, JASCO FT/IR-300E) in the wave number region 400–4000 cm⁻¹ collected at resolutions of 4 cm⁻¹. Commercial hydroxyapatite (Seikagaku Corp.) was used as a control.

3. Results and discussion

3.1. Apatite formation in R-SBF

Zhao and Gao recently reported that hydroxyapatite nanoparticles decorated on the sodium dodecyl sulfate (SDS) adsorbed MWNTs by an in situ synthetic method with calcium nitrate, Ca(NO₃)₂, and ammonium secondary phosphate, (NH₄)₂HPO₄ [18]. In contrast, our strategy for the apatite formation consists of biomimetic coating on the surface of MWNTs in the calcium phosphate solutions such as a SBF.

To optimize this strategy, we first studied the apatite formation on MWNTs in R-SBF. After immersion for 2 weeks, the MWNTs apparently became the gray in the solution. SEM images show the massive growth of the clusters of apatite crystallites with a needle-like shape on the aggregated MWNTs (Fig. 2A). Acicularly grown crystallites with about 150 nm in diameter form the bloom-shape morphology. A further detailed observation clearly showed that the crystallites of 100 nm in

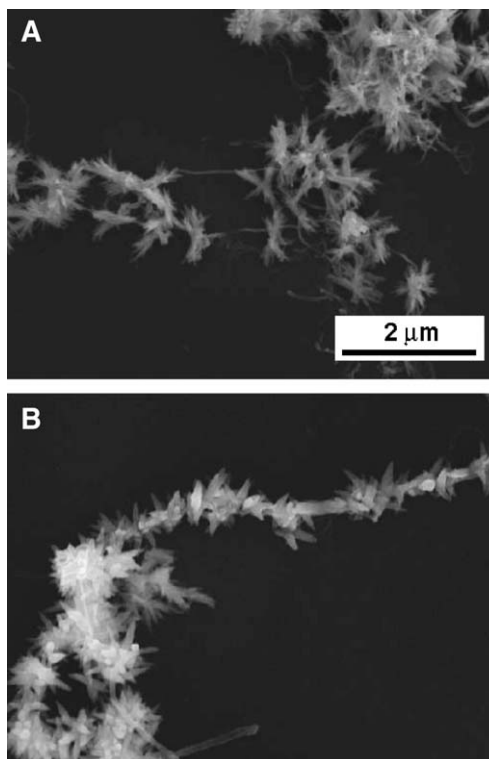


Fig. 2. SEM images of apatites: (A) needle crystallites grown radially on MWNT core; (B) barbed wire shape of crystallites on a MWNT core.

width and 200–500 nm in length were grown radially originating from a common center in the middle of a single MWNT and perpendicularly to the longitudinal direction of MWNT. In part, there exist bowknot-like bundles with their two ends fanning out while the middle part tying together [19]. Barbed wire-like-shaped feature in Fig. 2B was also observed.

From these results, the needle-like apatite crystallites were directly grown starting from the surface of MWNT. Thus, the MWNT may be acting as core for initial crystallization of the apatites. However, in this condition, the reproducibility of sizes and shapes of apatites formed on MWNTs was poor because R-SBF was highly supersaturated and was difficult to handle.

Fig. 3 shows the infrared transmission spectra of the apatite/MWNTs after immersion in R-SBF for 2 weeks. Compared with the spectrum of commercial hydroxyapatite as a control, very similar peaks at around 3440, 1099, 1040, 966, 607 and 569 cm⁻¹ on the spectrum were observed. The bands at 3440

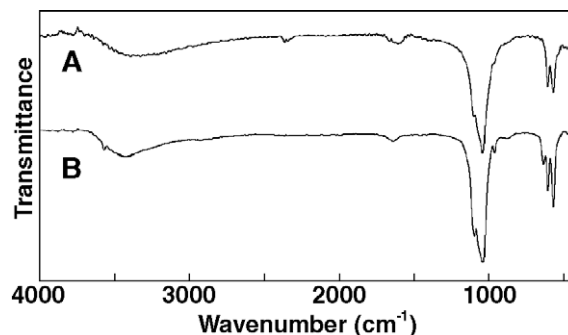


Fig. 3. FT-IR spectra of the apatite/MWNTs after immersion in R-SBF for 2 weeks (A) and hydroxyapatite as a control (B).

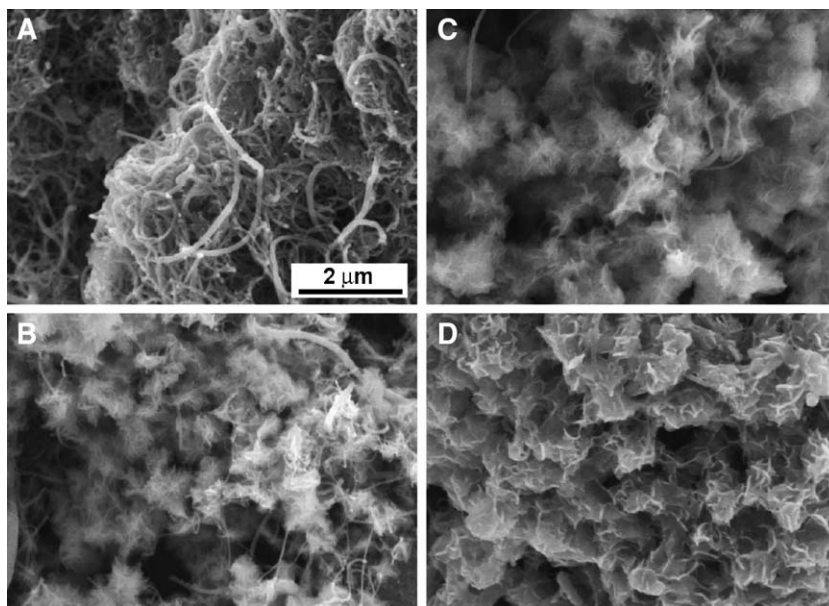


Fig. 4. SEM images of the apatite/MWNTs in PBS(+) after immersion for 6 h (A), 1 day (B), 2 days (C), and 2 weeks (D).

cm^{-1} and 1640 cm^{-1} may come from lattice H_2O . The phosphate modes 1046 cm^{-1} ($\nu_3(\text{PO}_4)$), 1029 cm^{-1} ($\nu_3(\text{PO}_4)$), 959 cm^{-1} ($\nu_1(\text{PO}_4)$), 590 cm^{-1} ($\nu_4(\text{PO}_4)$), and 577 cm^{-1} ($\nu_4(\text{PO}_4)$) are observed. However, no peaks were observed at 3536 and 633 cm^{-1} , which exist in the commercial hydroxyapatite and assigned to $-\text{OH}$ stretch and $-\text{OH}$ liberation, respectively. The spectrum of hydroxyapatite clearly shows the bands corresponding to hydroxyl groups. The spectrum of the apatite/MWNTs formed in R-SBF was similar to that reported by Harrison et al. [20] and may be composed of partly fluoridated apatite [21,22].

3.2. Influence of the time-course and substrate changes in PBS(+)

Fig. 4 presents the SEM images of the apatite/MWNTs after immersion in PBS(+). With the increase of immersion time (1 day to 2 weeks), the size of apatite crystallites increased. The growth on the MWNTs started with a nano-sized flake-like crystallite on 1 day (Fig. 4B) and followed by a constant growth during 2 weeks. The morphology was changed to the thicker leaf flake-like shape. After 2 weeks, the apatite crystallites showed the complete coverage over the aggregate of MWNTs (Fig. 4D). There was some incubating time for apatite nucleation. SEM did not observe apatite formation on surface up to 6 h immersion on the MWNTs treated with PBS(+) (Fig. 4A). Once the apatite nuclei are formed, they can grow spontaneously by consuming calcium and phosphate ions from PBS(+), since PBS(+) is already highly supersaturated with respect to apatite.

On the other hand, the immersion of MWNTs in S-SBF showed no apatite formation after 2 weeks (data not shown here). The S-SBF was stable without the precipitation during immersion for up to 2 weeks, while both R-SBF and PBS(+) were unstable. For nucleation to occur, an activation energy barrier must be exceeded. This activation energy can be

decreased by increasing the degree of supersaturation of calcium phosphate solutions. Thus, in the strategic point of view to modify MWNTs surface, it is effective to immerse in the higher supersaturated solutions as R-SBF or PBS(+).

The apatite formation in PBS(+) after a 2-week immersion was compared using SEM on both carbon plate and MWNTs substrates. Carbon plate substrate showed much less apatite formation sites than MWNTs. The few apatites formed on the carbon plate near its edge have a similar morphology as those formed on the MWNTs surface (Fig. 5). The results indicated

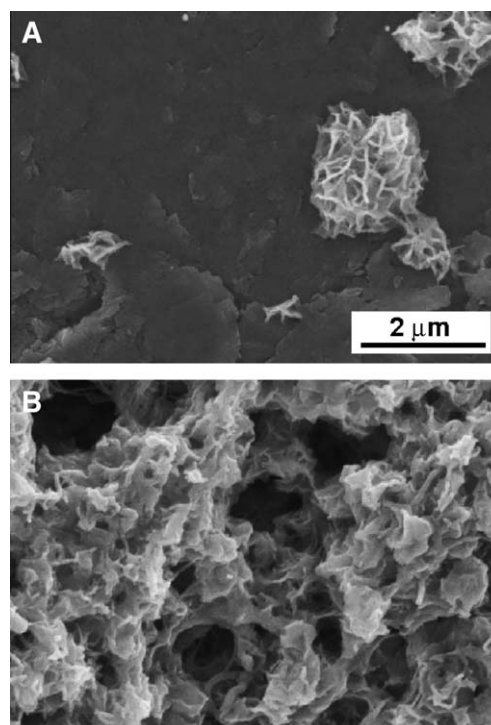


Fig. 5. SEM images of the apatites precipitated on carbon plate (A) and MWNTs in PBS(+) after 2 weeks (B).

that MWNTs have the stronger affinity for nucleation than carbon plate.

4. Conclusions

A simple route was developed to synthesize the apatite/MWNTs using the higher supersaturated calcium phosphate solution at ambient conditions. We obtained the apatites on the MWNT surface with different size and morphology within 2 weeks. The nano-sized apatite crystallites were produced in R-SBF for 2 weeks with a width of about 100–200 nm and a length of about 200–500 nm. The comparison of the apatite formation on both carbon plate and MWNTs substrates revealed significant differences in the density of apatite crystallites. The MWNT substrate showed much apatite formation more favorable than carbon plate. The results indicated that the MWNT acts as an effective nucleation surface to induce the formation of a biomimetic apatite coating. MWNTs with the defined surface morphology of nano apatite crystallites could be useful as biomaterials for scaffolds and for the biomedical applications.

Acknowledgements

This study was supported by Grant-in-Aid for Research on Nano-Medicine H14-nano-021 from Ministry of Health, Labor and Welfare of Japan.

References

- [1] A. Hirsch, *Angew. Chem., Int. Ed. Engl.* 41 (2002) 1853.
- [2] J.L. Bahr, J.M. Tour, *J. Mater. Chem.* 12 (2002) 1952.
- [3] Y.P. Sun, K. Fu, Y. Lin, W. Huang, *Accounts Chem. Res.* 35 (2002) 1096.
- [4] B. Fugetsu, S. Satoh, T. Shiba, T. Mizutani, Y. Nodasaka, K. Yamazaki, K. Shimizu, M. Shindoh, K. Shibata, N. Nishi, Y. Sato, K. Tohji, F. Watari, *Bull. Chem. Soc. Jpn.* 77 (2004) 1945.
- [5] B. Fugetsu, S. Satoh, A. Iles, K. Tanaka, N. Nishi, F. Watari, *Analyst* 129 (2004) 565.
- [6] K. Tamura, N. Takashi, T. Akasaka, I.D. Rosca, M. Uo, Y. Totsuka, F. Watari, *Bioceramics* 16 (2004) 919.
- [7] K. Tamura, N. Takashi, R. Kumazawa, F. Watari, Y. Totsuka, *Mater. Trans.* 43 (2002) 3052.
- [8] A. Yokoyama, Y. Sato, Y. Nodasaka, S. Yamamoto, T. Kawasaki, M. Shindoh, T. Kohgo, T. Akasaka, M. Uo, F. Watari, K. Tohji, *Nano Lett.* 5 (2005) 157.
- [9] S.C. Tsang, Z. Guo, Y.K. Chen, M.L.H. Green, H.A.O. Hill, T.W. Hambley, P.J. Sadler, *Angew. Chem., Int. Ed. Engl.* 36 (1997) 2198.
- [10] C.V. Nguyen, L. Delzeit, A.M. Cassell, J. Li, J. Han, M. Meyyappan, *Nano Lett.* 2 (2002) 1079.
- [11] W. Huang, S. Taylor, K. Fu, Y. Lin, D. Zhang, T.W. Hanks, A.M. Rao, Y.P. Sun, *Nano Lett.* 2 (2002) 311.
- [12] M. Shin, N.W.S. Kam, R.J. Chen, Y. Li, H. Dai, *Nano Lett.* 2 (2002) 285.
- [13] T. Akasaka, K. Matsuura, N. Emi, K. Kobayashi, *Biochem. Biophys. Res. Commun.* 260 (1999) 323.
- [14] T. Akasaka, K. Matsuura, K. Kobayashi, *Bioconjug. Chem.* 12 (2001) 776.
- [15] H.-M. Kim, T. Miyazaki, T. Kokubo, T. Nakamura, *Key Eng. Mater.* 192–195 (2001) 47.
- [16] A. Oyane, M. Kawashita, K. Nakanishi, T. Kokubo, M. Minoda, T. Miyamoto, T. Nakamura, *Biomaterials* 24 (2003) 1729.
- [17] W.-W. Song, Y.-K. Jun, Y. Han, S.-H. Hong, *Biomaterials* 25 (2004) 3341.
- [18] L. Zhao, L. Gao, *Carbon* 42 (2004) 423.
- [19] J. Liu, K. Li, H. Wang, M. Zhu, H. Yan, *Chem. Phys. Lett.* 396 (2004) 429.
- [20] J. Harrison, A.J. Melville, J.S. Forsythe, B.C. Muddle, A.O. Trounson, K.A. Gross, R. Mollard, *Biomaterials* 25 (2004) 4977.
- [21] Q. Williams, E. Knittle, *J. Phys. Chem. Solids* 57 (1996) 417.
- [22] L.M. Rodriguez-Lorenzo, J.N. Hart, K.A. Gross, *Biomaterials* 24 (2003) 3777.